8. Ultraviolet Absorption

Experiment MA-059*

T. M. Donahue,[a†] R. D. Hudson,[b†] W. T. Rawlins,[c] J. Anderson,[a] F. Kaufman,[c] and M. B. McElroy[d]

ABSTRACT

The Ultraviolet Absorption Experiment performed during the Apollo-Soyuz mission involved sending a beam of atomic oxygen and atomic nitrogen resonance radiation (130.4 and 120.0 nm), strong unabsorbable oxygen and nitrogen radiation (130.6 and 149.3 nm), and visual radiation, all filling the same 3°-wide field of view from the Apollo to the Soyuz. The radiation struck a retroreflector array on the Soyuz and was returned to a spectrometer onboard the Apollo. Lock on the retroreflector was maintained by the visual light and a star tracker. The density of atomic oxygen and atomic nitrogen between the two spacecraft was measured by observing the amount of resonance radiation absorbed when the line joining Apollo and Soyuz was perpendicular to their velocity with respect to the ambient atmosphere. By allowing the Apollo spacecraft to drift at fixed ranges of 150, 500, and 1000 m through an arc of ±15° with respect to the perpendicular to the velocity vector, the temperature of the gas was obtained; i.e., the Doppler line profile was scanned. Information concerning oxygen densities was also obtained by observation of resonantly fluorescent light. The absorption experiments for atomic oxygen and atomic nitrogen were successfully performed at a range of 500 m, and abundant resonance fluorescence data were obtained.

INTRODUCTION

The Ultraviolet Absorption (UVA) Experiment is one of the five experiments that incorporated joint activities between the U.S. and U.S.S.R. crews during the Apollo-Soyuz Test Project (ASTP) mission. The experiment provided an opportunity for the realization of a technique devised to permit the measurement of atmospheric species concentrations. This experiment involved the application of the most reliable and specific laboratory technique available for measuring the concentration of a given gaseous species—atomic absorption spectroscopy. This method is probably the most reliable available tool for quantitative analysis if the cross sections or oscillator strengths for absorption are known, if proper precautions are taken to ascertain the frequency dependence (or line shapes) of light sources and absorbers, if optical properties of the measuring devices are measured, and if corrections are made for absorption by other species (or impurities). A complementary technique, the quantitative observation of resonance fluorescence in which atomic or molecular species scatter resonance radiation from a light source into a detector, is a powerful one and was used in the ASTP UVA experiment. The species chosen for detection and measurement were neutral atomic

*The joint U.S.-U.S.S.R. designation was "Experiment AS-5."

[a]University of Michigan.

[b]NASA Goddard Space Flight Center.

[c]University of Pittsburgh.

[d]Harvard University.

†Co-Principal Investigator.

oxygen (O) and neutral atomic nitrogen (N). The first was selected for several reasons.

1. Strong resonance light sources are available that produce radiation in the resonance triplet at 130.2, 130.5, and 130.6 nm, hereafter referred to as 130.4-nm radiation.

2. The absorption cross section or oscillator strength of O for the energy-state transition producing or absorbing this radiation ($^3P_{2,1,0}$ $^3S_1$) is accurately known.

3. Although O is the most abundant atmospheric species at the experiment altitude (225 km), to detect the species cleanly in a mass spectrometer is difficult because of its propensity to recombine into molecular oxygen (O_2) upon colliding with the walls of a spectrometer ion source. At lower altitudes, this recombination has caused difficulties that leave the actual density of O near 120 km uncertain by a factor of 5 or more. At an altitude of 225 km, the uncertainty is probably not very great, but it is interesting to attempt to verify other measurement methods by a new one or to prove the new method by comparison with ground truth.

Atomic nitrogen was interesting because, as of a year or so ago, the direct measurement of this species in the thermosphere had probably not yet been performed successfully. A satellite mass spectrometer result (ref. 8-1) obtained at an altitude of 400 km suggested that the partial pressure of N exceeded that of molecular nitrogen (N_2), but the result was flawed by low mass resolution. A rocketborne mass spectrometer result by Ghosh and others (ref. 8-2) suggested that, at an altitude of 185 km, the density of N was 6 percent that of N_2, although Hickman and Nier (ref. 8-3) showed that this is an upper limit.

The problems in measuring N mass spectrometrically are similar to those of obtaining O measurements but are more serious because the density ratio of N to N_2 in the thermosphere is small. The N_2 can be dissociatively ionized in the spectrometer ion source; like O, N is highly reactive and can recombine not only to form N_2 on instrument chamber walls but can form other compounds such as NO.

PRINCIPLE OF THE UVA EXPERIMENT

The principle of the UVA measurement was to produce fairly well collimated beams of 130.4- and 120.0-nm radiation (resonance for O and N), and 135.6- and 149.3-nm radiation (forbidden lines of O and N that are very weakly absorbed by these species). The forbidden line radiation originated in the same sources as the resonant line radiation and hence defined the beam geometry, the reflectivity, and the transmission of the optical instrument for the resonance radiation independently of resonance absorption. The light was produced by radiofrequency-driven lamp sources and collimated by mirrors on the Apollo spacecraft. The light beams illuminated an array of corner reflectors mounted on the Soyuz spacecraft at a known distance x from the Apollo UVA light source. Thus, the portion of the beam striking the retroreflectors returned to a collecting mirror near the Apollo collimating mirror. From this mirror array, the radiation was focused on the entrance slit of a 0.75-m Ebert-Fastie scanning spectrophotometer by an auxiliary mirror. The spectral range from 120.0 to 149.3 nm was scanned every 12 seconds through 1.5-nm ranges centered on 120.0, 130.4, 135.6, and 149.3 nm. The bandwidth of the spectrometer was approximately 1.15 nm. The spectrometer was a modified backup unit for the one used on the Apollo 17 experiment (ref. 8-4).

In its simplest terms, the principle of the UVA experiment is illustrated in figure 8-1. A known flux of resonance radiation F is radiated into a solid angle Ω. At a distance x from the source, the

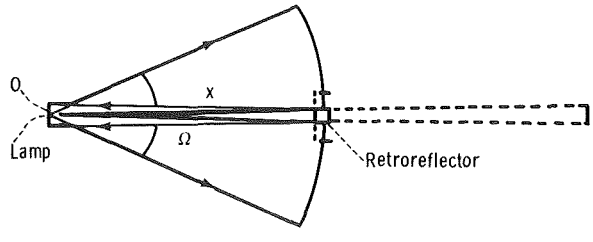

FIGURE 8-1.—Basic geometry of the UVA experiment.

irradiance is $F/\Omega x^2$. If the reflectivity of each surface of the retroarray is r and the retroarray surface area is A, an amount of radiation $r^3FA/\Omega x^2$ is returned to point O and passes through a well-defined and limited region determined by the shape of the collimating mirror, the shape of the corner reflectors, and the geometry of the retroreflector array. Essentially, light from each point on the collimating mirror that strikes a given retroreflector returns through a region of the same shape but twice the linear dimensions of the corner reflector. The pattern of light sent from a point source to a corner reflector that is a distance x from the source and back to the source is analogous to the pattern of light sent from the point source to a hole in an opaque screen at a distance x of the same shape as the reflector and then on through the aperture to a screen that is a distance $2x$ from the source. If a fraction of this returned light f is sent to a spectrometer having a throughput QT, where Q is the quantum efficiency and T is the transmission, the counting rate R of a detector in the spectrometer will be

$$R = r^m \frac{FA}{\Omega x^2} \exp(-2\bar{\sigma} xn) fQT \qquad (8\text{-}1)$$

where m is the number of reflections, six in the present case; $\bar{\sigma}$ is the mean absorption cross section; and n is the attenuation coefficient. Obviously, r is assumed to be the same at each surface for a given wavelength.

The flux F of 130.4-nm radiation was 5×10^{13} photons/sec into a solid angle Ω of 0.75 sr. Typical values for the other terms in the equation are as follows.

$$\begin{aligned} r &= 0.75 \\ m &= 6 \\ A &= 55 \text{ cm}^2 \\ f &= 0.2 \\ T &= 0.2 \\ Q &= 0.12 \text{ electron/photon} \\ \bar{\sigma} &= 10^{-13} \text{cm}^2 \end{aligned}$$

Thus

$$R \approx 3 \times 10^{12} x^{-2} \exp(-2\bar{\sigma} xn) \qquad (8\text{-}2)$$

The unattenuated counting rate R_0 is $3 \times 10^{12} x^{-2}$, or 3×10^2 counts/sec even at a range of 1 km. It was assumed that the minimum absorption that could be detected was 10 percent; i.e., $\exp(-2\bar{\sigma} xn) = 0.9$, or $xn = 2 \times 10^{12}$ cm^{-2}. Thus, at 100 m, an absorber density of 2×10^9 cm^{-3} should be detectable and, at 1 km, a density of 2×10^7 cm^{-3} should be detectable. In this case, the counting rate will be 270 counts/sec, compared with the unabsorbed rate of 300 counts/sec.

In an experiment such as this, the spacecraft velocities are greater than the average thermal velocities of the gas particles at 1000 K (by a factor of 8 for oxygen). Hence, the frequency of the lamp signal will be shifted far away from the absorption frequency of the atoms by the Doppler effect if the light is radiated in the approximate direction of the Apollo velocity vector. It is therefore necessary to conduct the experiment with the vector between the spacecraft nearly perpendicular to the spacecraft velocity vectors. A simple calculation shows that, if the angle between the direction of emission of the light signal and the Apollo velocity vector were 78° with the two spacecraft 100 m apart, the absorption by 4×10^9 atoms/cm^3 of oxygen would be only 30 percent compared to 82 percent if the angle were 90°. This effect could, however, readily be turned into an advantage if the experiment were performed in such a way that one spacecraft (for example, Apollo) slowly drifted past the other at a fixed range and the angle between them varied through approximately 30° centered on the normal to the orbital velocity vector. The reasons are twofold. First, it would not be necessary to determine by some independent measurement when the angle of observation was 90° to the direction of the relative wind. This information would automatically be determined as the point at which the counting rate became minimum. Second, the change in counting rate with angle would define the Doppler line shape of the absorbing atom. Hence, the functional form of this variation would enable measuring the temperature of the absorbing atoms.

In practice, it is necessary to consider the fact that the light flux F varies with wavelength λ for each fine structure component of the resonance lines, and that the absorption cross section σ is

also a function of wavelength. Thus, the term $F\exp(-2\bar{\sigma}\, nx)$ in equation (8-1) must be replaced for each fine structure component by

$$\int_i F_i\,(\lambda)\exp[-2\,xn\sigma(\lambda)]\,d\lambda \tag{8-3}$$

where $F_i(\lambda)$ depends on the effective lamp temperature T_L and $\sigma(\lambda)$ values depend on the gas temperature T_G. When there is no relative motion between source and absorber, the functional form of $F(\lambda)$ may be written

$$\left(\frac{mc^2}{2\pi kT_L\lambda_{0i}^2}\right)^{1/2}\exp\left[\frac{-mc^2\left(\lambda-\lambda_{0i}\right)^2}{2kT_L\lambda_{0i}^2}\right] \tag{8-4}$$

where λ_{0i} is the line center wavelength of the i-th fine structure component, m is the atomic mass of the gas species, c is the speed of light, and k is the Boltzmann constant. When u is the component of the atmospheric velocity along the light beam in the coordinate system in which the Apollo vehicle is at rest, $\sigma(\lambda)$ becomes

$$\sigma_0\exp\left\{\frac{-mc^2\left[\left(\lambda-\lambda_0\right)c-u\lambda_0\right]^2}{2kT_G\lambda_0^2c^2}\right\} \tag{8-5}$$

Finally, because the spectrometer does not resolve the fine structure components in the spectrum, it is necessary to sum over fine structure components to obtain the predicted counting rate.

$$R=\Sigma R_i \tag{8-6}$$

The spectral parameters for the gases involved in this experiment are shown in table 8-I.

Figures 8-2(a) and 8-2(b) show the counting rates as a function of spacecraft separation when $u=0$ for O and N, respectively, at typical gas concentrations. Figures 8-3(a) and 8-3(b) show, for various values of T_G, the variation in atmospheric transmission as a function of the angle θ between the direction of observation and the perpendicular to the wind velocity vector in the coordinate system in which the Apollo spacecraft is at rest. The lamp output (integrated over wavelength of all spectral components) is assumed to be 10^{13} photons/sec for the oxygen 130.4-nm triplet and 3×10^{12} photons/sec for the nitrogen 120.0-nm triplet.

A practical complication is introduced in performing this experiment because the resonance radiation in the emitted beam can be scattered resonantly by the gas to be studied. Some of this radiation will be emitted in a direction to enter the spectrometer slit, although it is a relatively small amount of the total scattered light because the scattering is virtually isotropic. If one considers the light traveling in a certain direction from the light source (treated as a point source) and calls the number of photons crossing unit area per second at a distance x from the source $I_L(\lambda)$, the number of these scattered per second will be

$$\int_{x_0}^{\infty}\int_0^{\infty} I_L(\lambda)n\sigma(\lambda)\exp\left[-2n\int_0^x\sigma(\lambda)dx'\right]d\lambda\,\frac{dx}{4\pi x^2} \tag{8-7}$$

where x_0 is the distance from the light source at which the outgoing beam crosses the spectrometer field of view. To evaluate the actual counting rate due to these scattered photons, it is necessary to evaluate the overlap of the outgoing beam with the effective spectrometer field of view. For example, the field of view is filled gradually and not abruptly at a distance x_0 along the beam. This evaluation is being conducted for the instrument

actually flown. A reasonable approximation for the counting rate from resonance fluorescence R_F is

$$R_F = \frac{FA_M A_{SM} A_S r^3 QT}{4\pi p^2 \Omega} \int_{x_0}^{\infty} \frac{dx'}{x^2}$$

$$\int_0^{\infty} I_L(\lambda) n(x) \sigma(\lambda) \exp\left[- \int_0^{x} 2n\sigma(\lambda) dx \right] d\lambda \qquad (8\text{-}8)$$

where

A_M = the lamp collimating mirror area (3.3 by 5.7 cm)

A_{SM} = the area of the collecting mirror (5.5 by 3.7 cm)

A_S = the area of the spectrometer slit (0.2 by 5.7 cm)

p = the focal length of the collecting mirror (16.5 cm)

x_0 = 75 cm

The contribution of resonance fluorescence under the same conditions assumed in the absorption calculation is shown in figure 8-2. The fluorescence contribution varies with the angle between

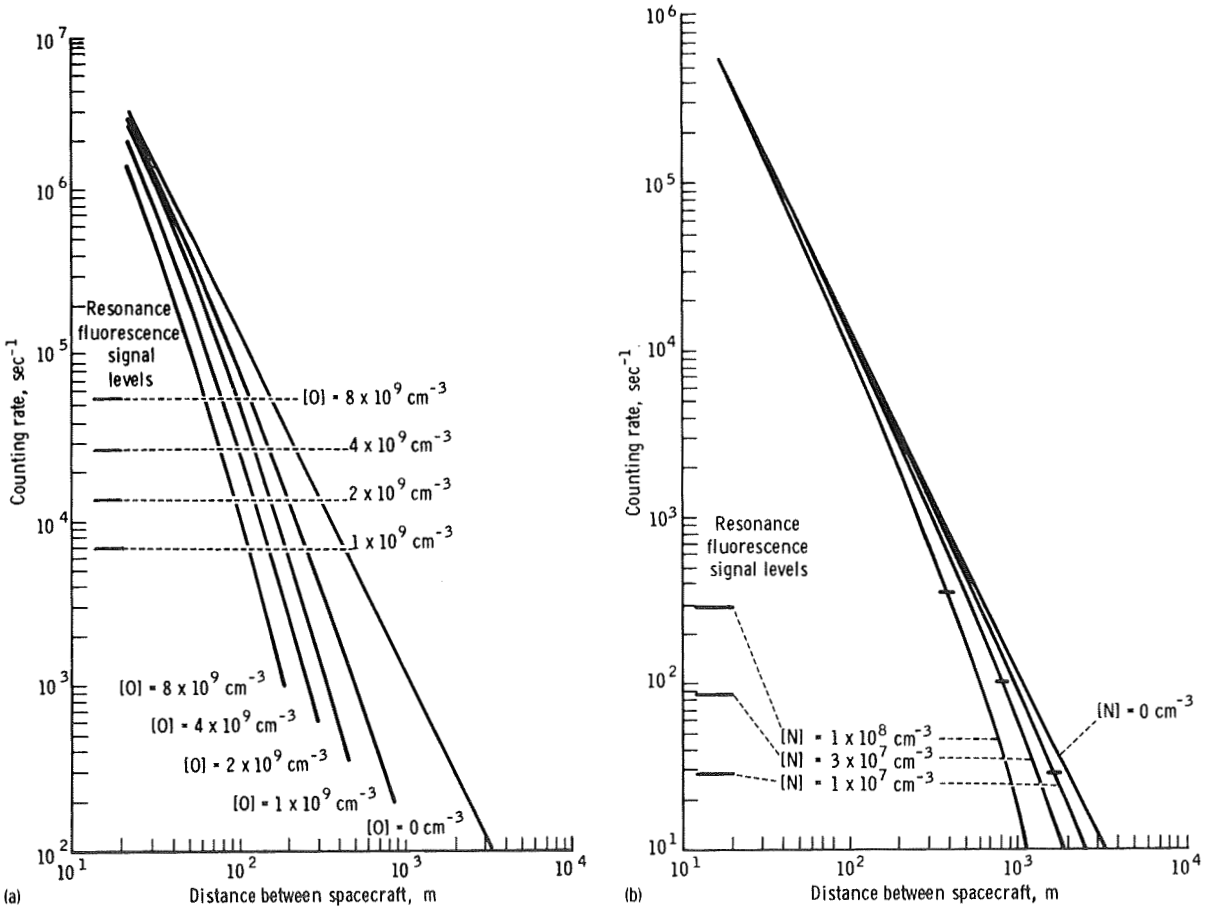

FIGURE 8-2.—Spectrometer signal as a function of spacecraft separation distance (where [O] and [N] are the density of oxygen and nitrogen, respectively). (a) Oxygen atoms. (b) Nitrogen atoms.

direction of observation and velocity vector and reaches a maximum where the transmitted light reaches a minimum; i.e., when the wind velocity component in the direction of observation is zero. The resonance fluorescence contribution to the observed counting rate as a function of time (or angle) must be evaluated independently so that it can be subtracted from the total counting rate to obtain the contribution due to transmitted (or absorbed) radiation alone; also to be subtracted are background signals from airglow.

The heart of the experimental apparatus is the Apollo 17 Ebert-Fastie spectrometer. It was equipped with a new grating drive cam that rotated the grating to scan from 129.65 to 131.15 nm in 2.5 seconds, from 119.25 to 120.75 nm in 4.5 seconds, from 129.65 to 131.15 nm again in 2 seconds, from 134.85 to 136.35 nm in 1.25 seconds, and from 148.55 to 150.05 nm in 1.25 seconds. The light output of each lamp was pulsed with a pulse duration of 0.1 second; the sequence was the O lamp alone, the N lamp alone, and both lamps off.

The resonance lamp light sources, the retroreflector array, and the optical transmitting and receiving systems had to be designed around the spectrometer in such a way as to maximize the signals received. The spectrometer choice was governed by availability and by the schedule for experiment preparation. The instrument has an entrance slit of 0.2 by 5.7 cm, with an f/5 collecting aperture corresponding to a solid angle of 12° by 12°. The ultraviolet lamps have a 1-cm source diameter and emit into a solid angle of approximately 56° full width, or 0.74 sr. The flux from each lamp is collimated by a mirror placed 12 cm from the lamp. Because the source diameter in the lamps is 1 cm, the beam leaves the collimating mirror with a spread of approximately 5°.

In designing the corner reflector array, it was necessary to consider that the optimum diameter of the mirror that focuses the returned light on the spectrometer slit equals the width of an individual corner reflector. The corner reflectors must be packed efficiently into an array of convenient diameter. The arrangement adopted was a 10-cm array diameter, and each reflector was 3.3 cm wide (fig. 8-4). In this case, the focusing mirror diameter was 3.3 cm, and the mirror was placed 16.5 cm from the slit to fill the slit aperture laterally.

TABLE 8-I.—Spectral Parameters for Atmospheric Absorption Experiment

Species	*Spectral line, nm*	*Absorption cross section at 300 K (σ_0), cm^2 (a)*	*Relative lamp intensity F_i*	*Relative atmospheric populations at 1050 K*
O	130.217	1.6×10^{-13}	0.542	[b]0.613
	130.487	1.6	.337	[b].297
	130.601	1.6	.120	[b].090
N	119.955	3.8	.500	1.000
	120.022	2.5	.333	1.000
	120.071	1.3	.167	1.000

[a]$\sigma_0(T_G) = \sigma_0(300\text{ K})\sqrt{300/T_G}$. The values of $\sigma_0(300\text{ K})$ are calculated from the oscillator strengths given in reference 8-5.

[b]The relative atmospheric populations for atomic oxygen are calculated from the following formulas.

$$n_{130.2}/n_{\text{total}} = 5/(sum)$$

$$n_{130.5}/n_{\text{total}} = \left[3\exp\left(-228.24/T_G\right)\right]/(sum)$$

$$n_{130.6}/n_{\text{total}} = \left[\exp\left(-326.16/T_G\right)\right]/(sum),$$

where $(sum) = 5 + \left[3\exp\left(-228.24/T_G\right)\right] + \left[\exp\left(-326.16/T_G\right)\right]$

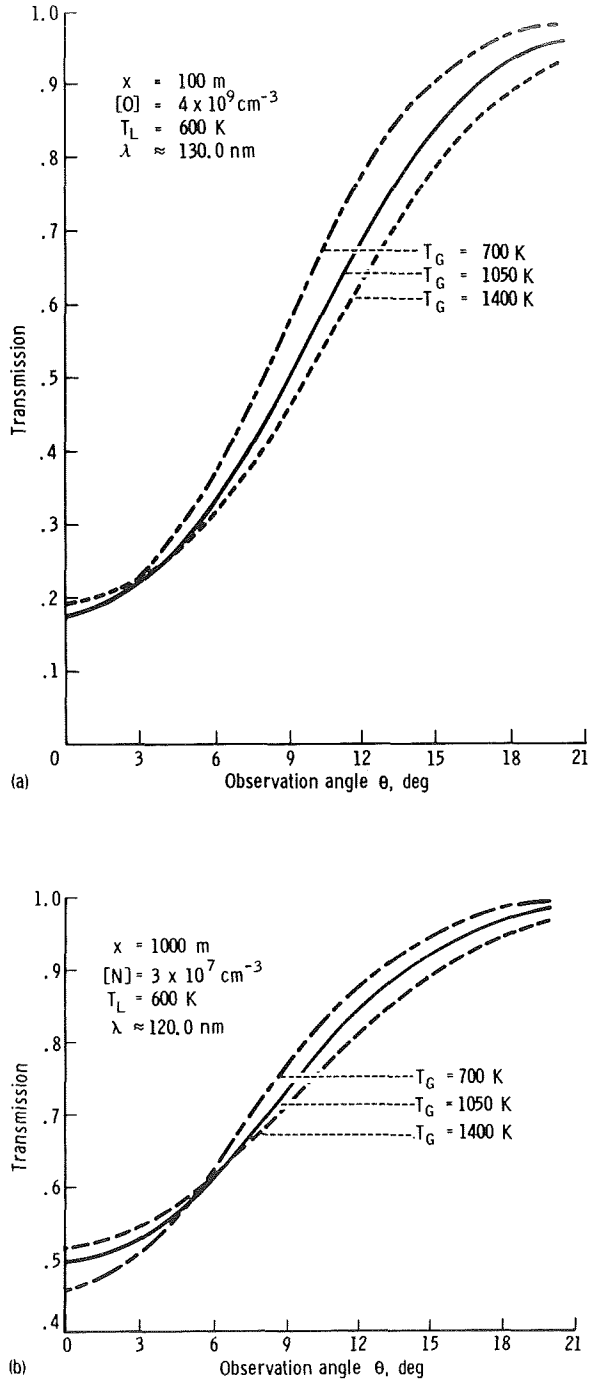

FIGURE 8-3.—Variation of atmospheric transmission as a function of the observation angle. (a) Oxygen atoms. (b) Nitrogen atoms.

The geometry of the optical transmitting and collecting system is defined in figure 8-5. Light originating from a point on a collimating mirror will return from the corner reflector and pass through a region centered at that point on the mirror but twice as large in linear dimensions as the corner reflector (neglecting diffraction effects). For example, light originating from point x on the O mirror in figure 8-6 will return through the 6.6-cm dashed-line region (hexagonal). It is reasonable to put the collecting mirror in the space bounded by the collimating mirrors and allow the dimensions to be 3.3 by 5.7 cm. The contribution to the collected light originating from point x is then the shaded overlap of the collecting mirror and the hexagonal area 6.6 cm in diameter and centered at point x. The size of the return beam from all points on the collimating O mirror is shown by the broken line. The collecting mirror must be protected from stray light coming from the lamps by means of baffling because the most intensely illuminated region is that adjacent to the collimating mirror.

Figure 8-7 shows how the fluorescence and transmitted signals should vary with wavelength around 130.4 nm. This calibration was done by convoluting the previously computed signal intensities in each of the three components of the oxygen triplet with the spectrometer slit function. The latter was assumed to be triangular with a full width of 1.15 nm at half maximum. The case shown is for an Apollo-Soyuz separation of 100 m, an oxygen density [O] of 4×10^9 cm^{-3}, a lamp temperature T_L of 600 K, and a gas temperature T_G of 1050 K. The curves are normalized. The difference in wavelength at the peak occurs because most of the transmitted signal is in the weaker 130.5- and 130.6-nm components, whereas most of the fluorescence signal is from the 130.2-nm line.

A third light source was incorporated in the apparatus to provide bright visual light illuminating the same field of view as the ultraviolet sources. The collimating lamp, marked "Visible" in figure 8-6, provided input to a star tracker with output in the spacecraft to indicate to the astronaut whether the retroreflector array was being illuminated by the lamp beams, and, more importantly, whether the retroarray was in the spectrometer field of

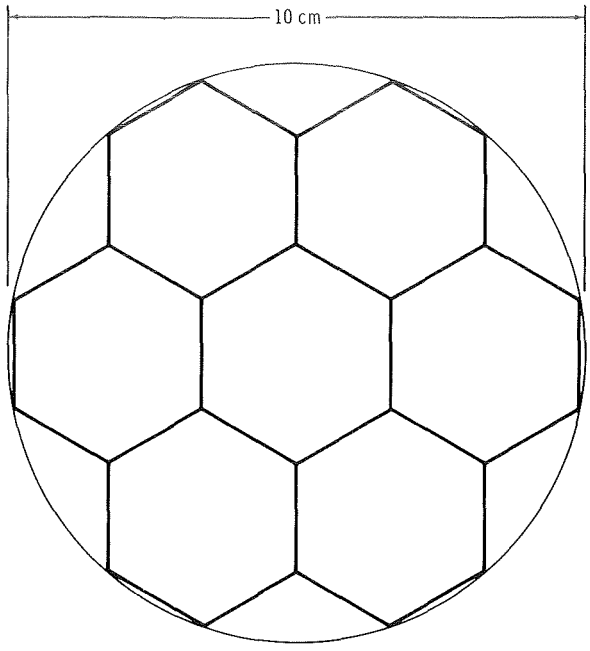

FIGURE 8-4.—Arrangement of mirrors in the retroreflector array.

view (±0.35° in pitch). A backup to the star tracker was provided by the crew optical alinement sight (COAS), through which the retroreflector could be seen. The COAS was provided with a reticle marked in degrees in the pitch and yaw directions.

A door was provided that was closed when data were not being taken. The inside surface of the door was blackened. However, small reflecting cylinders, one for each of the ultraviolet sources, were fitted in the door. These cylinders provided a means of in-flight calibration. The counting rate as a function of grating position was obtained with the flight unit during thermal-vacuum (TV) checks of the instrument for comparison with calibration runs made during flight.

The reflectivity of the retroreflectors was measured as a function of wavelength. The transmission T of the full receiving system, the external optics, and the telescope were also measured at the John Hopkins University with the cooperation of W. G. Fastie. The quantum

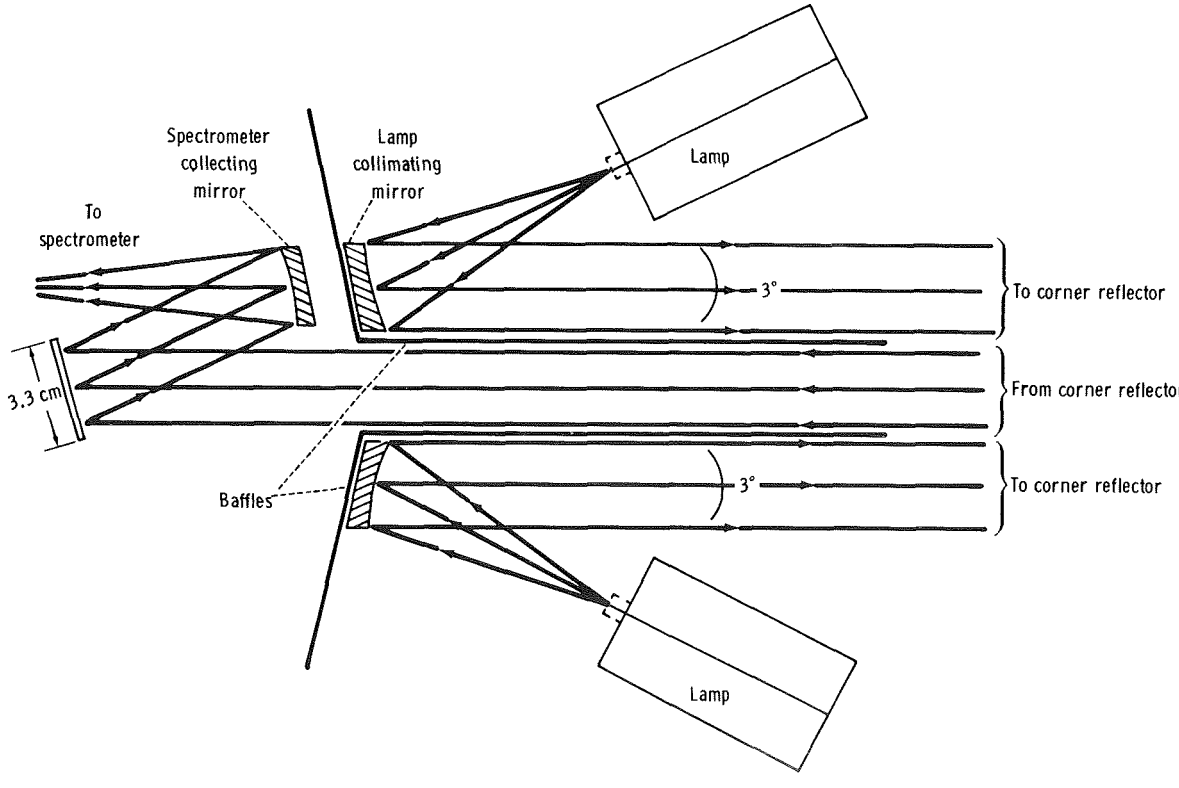

FIGURE 8-5.—Schematic diagram of optical transmitting and collecting system.

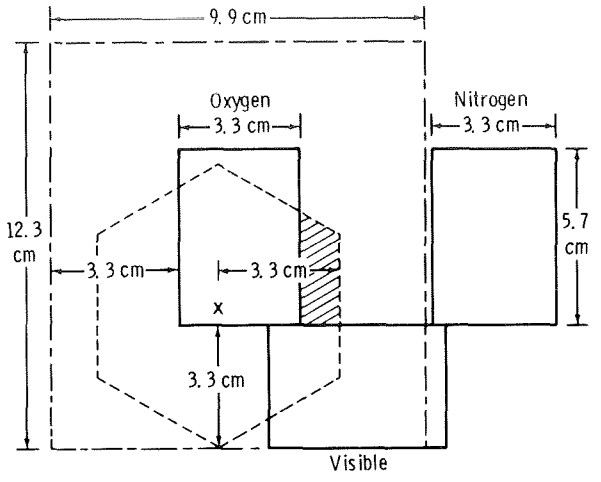

---- Return beam dimensions from single point on lamp mirror
—— Return beam dimensions from entire lamp mirror

FIGURE 8-6.—Geometry of return beam from the retroreflector array.

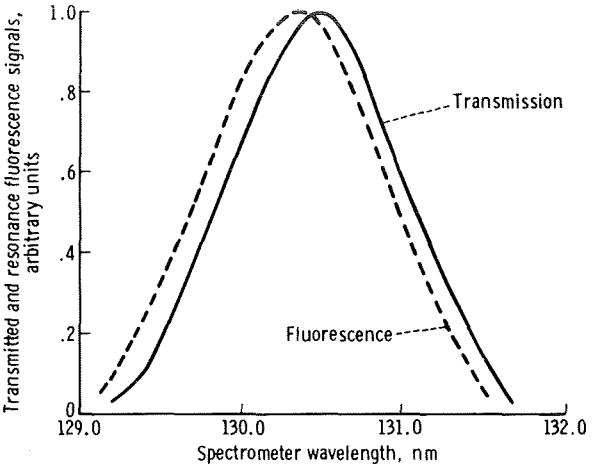

FIGURE 8-7.—Transmitted and resonance fluorescence signals as a function of spectrometer wavelength setting.

efficiencies of the detectors Q for both flight and backup units were also measured. Pertinent data are shown in tables 8-II to 8-V.

The flight lamps and backup lamps were calibrated to determine the flux of photons emitted. For this calibration, a monochromator and a double ionization chamber (for the 120.0- and 130.4-nm lines) were used, and a measurement of the photocurrent in the monochromator detector (for the 135.6- and 149.3-nm lines) was made. The data obtained for the flight lamps were reduced to absolute intensities by comparison with similar measurements made with the same system on another lamp that had been absolutely calibrated at the University of Pittsburgh. The detector used at Pittsburgh to calibrate the standard lamp had been calibrated by a measurement of its response to radiation at the four wavelengths in question emitted from a beam of O and N atoms of known density excited by electron impact. The flux from the flight lamp is given in table 8-III.

The effective lamp temperatures T_L were also measured at the University of Pittsburgh by measuring the absorption of their resonance radiation by a column of atoms of known concentration at a temperature of 300 K. The surprising result was that typical effective temperatures for the oxygen lamps were very large, from 2200 to 3700 K. The high temperature is presumed to be caused by the presence of many atoms that have been dissociatively excited from O_2 into high radiating states of O, and have cascaded into the resonantly radiating state before undergoing many collisions. This was not the case for the nitrogen lamps. The flight lamp temperatures were 2500 K for the oxygen lamp and 400 K for the nitrogen lamp. The UVA experiment was mounted on the Apollo docking module with the field of view forward (plus-X axis).

RESULTS

The first exercises of the UVA experiment began when the lamps were turned on at 27:00 ground elapsed time (GET) on Wednesday, July 16, 1975. The counting rate as a function of cam position closely reproduced that obtained with the door closed in the last TV tests before the apparatus left the laboratory (table 8-IV). At 28:30 GET, the cover was opened and the spacecraft was pointed toward the star Vega. The purpose of this exercise was to calibrate the COAS and to test the star-tracker system designed to lock the field of view on a target. During this test, the obtaining of resonance fluorescence signals in the oxygen

TABLE 8-II.—Product of Quantum Efficiency and Transmission QT for Flight and Backup Units

Wavelength, nm	*Backup unit QT*	*Flight unit QT*
130.4	0.0258	0.0307
120.0	.0129	.0264
130.4	.0272	.0397
135.6	.0258	.0311
149.3	.0151	.0172

TABLE 8-III.—Flight Lamp Fluxes Into 0.74 sr

Flight lamp	*Wavelength, nm*	*Flux, photons/sec*
O	130.4	10.4×10^{13}
	135.6	1.78
N	120.0	.634
	149.3	1.45

TABLE 8-IV.—Comparison of Counting Rates for Flight and Backup Units

Wavelength, nm	*Activity, counts/sec, for -*			
	TV test of flight unit	*During flight with backup unit*	*Ratio flight/ TV test*	*Ratio QT backup unit/QT flight unit*
130.4	27 310	21 260	0.78	0.84
120.0	21 788	18 359	.84	.78
130.4	27 771	21 709	.78	.69
135.6	6 363	4 268	.67	.83
149.3	13 527	11 881	.88	.88

130.4-nm channels was verified. One problem was discovered, however; the star tracker indicated lock while the COAS indicated star movement from 3° to the right to 2.5° to the left. This difference occurred because a spacer was inserted between the lens and aperture of the star tracker to increase the size of the light spot on the photocathode and thereby to change the slope of the star-tracker response curve. This change moved the focal point approximately 0.25 cm in front of the aperture and enlarged the star-tracker field of view to the limits of the star-tracker tube, 5.5°, due to vignetting. To avoid operating with the retroreflector out of the field in yaw (even though the star tracker indicated it was in the field), the chart on the COAS reticle was marked at ±1.5° and the crew was instructed to prevent straying of the retroreflector image beyond these limits. In fact, the crew was asked to keep the retroreflector as near as possible to the center of the COAS.

Five additional data-taking exercises were performed. After the final undocking on July 19, 1975, the Apollo vehicle assumed a stationkeeping position 18 m ahead of the Soyuz vehicle as the two spacecraft approached the morning terminator. The UVA power was turned on at approximately 98:55 GET, 30 minutes before the first observational exercise, to permit stabilization of the lamps and the photomultiplier tube. During this period, calibration data were obtained using the door reflectors. Table 8-IV presents results for comparison with those obtained during the final TV tests conducted at the Applied Physics Laboratory of Johns Hopkins University. The counting rates during flight were approximately 0.8 of those obtained on the ground. This effect can be attributed to use of the detector head from the backup unit to replace that of the flight unit on the launch pad shortly before flight because of an electronics problem. A comparison of the ground-test product of *QT* values for the two units (table 8-IV) shows that the ratios are about the same as the flight to ground-based counting rate ratios. At 99:25 GET, the Soyuz crew activated circuits to unlatch covers over the Soyuz retroreflector arrays. Two arrays were mounted on top of the vehicle, one facing upward, and the other facing starboard. A third array was mounted on the rear of

TABLE 8-V.—Retroreflector Reflectivities

Wavelength, nm	*Reflectivity from -*	
	Aft	*Top*
130.4	0.60	0.57
120.0	.56	.54
135.6	.55	.52
149.3	.52	.49

the spacecraft facing aft. The Apollo crew verified with binoculars that the covers on the top-mounted retroreflectors had opened. (If the starboard array had not opened, a contingency plan would have permitted a Soyuz yaw so that its aft-mounted retroreflectors could be used in the experiment). Power to the UVA was briefly turned off while the door of the instrument was opened after the terminator had been passed. (The power-down precaution was necessary so that large flashes of light would not damage the detectors as the door was being opened or closed.) Beginning 18 minutes before the data-gathering run, the Apollo vehicle moved out of the orbital plane (fig. 8-8) until it was 150 m from the Soyuz vehicle and oriented so that the retroreflector could be illuminated. At this time, the angle between the perpendicular to the Soyuz velocity vector and the Apollo vehicle was 15°. The Apollo vehicle then was maneuvered through a 33° circular arc sweep passing through the normal to the velocity vector while the crew attempted to keep the retroreflector illuminated following procedures described previously. Both the star-tracker output and the COAS observations indicated that a lock was obtained. A problem occurred during the first several minutes of the run because the Soyuz flashing beacons and orientation lights were not extinguished. After the data-taking maneuver (lasting 10 minutes) was completed, the Apollo vehicle returned to a stationkeeping position 50 m from the Soyuz vehicle but facing in the direction of motion, as the Soyuz yawed 180° to face the Apollo.

For reasons still not understood, no clearly identifiable reflected ultraviolet radiation was detected during this pass. There was a strong 130.4-nm signal that was almost surely resonance fluorescence, but there were no counts above background in the 135.6-, 149.3-, or 120.0-nm channels. The Apollo crew reported that both the Soyuz window and the retroreflector were illuminated, and two possible explanations for failure were considered. One was that the reflectivity of the retroreflector had been seriously degraded during the flight. The other was that a window reflection was registered by the star tracker as a reflection from the retroreflector. The second explanation is not consistent with the fact that, through the COAS, an illuminated retroreflector was seen centered in the field of view. It was decided, therefore, not to risk using the side-looking retroreflector during the scheduled run at 500 m separation but to request performance of a Soyuz 90° yaw maneuver to enable use of the aft-looking reflector.

The procedure followed during the 500-m data take was very similar to that described at 150 m (fig. 8-9). It occurred during the next eclipse period. Calibration data with the door closed were obtained starting at 100:30 GET (about 35 minutes before the run). The Apollo vehicle

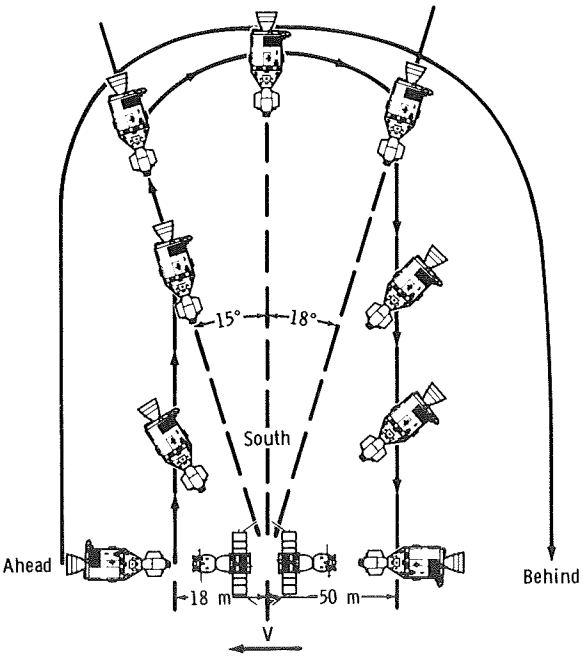

FIGURE 8-8.—Illustration of the 150-m out-of-plane data take (V= velocity vector).

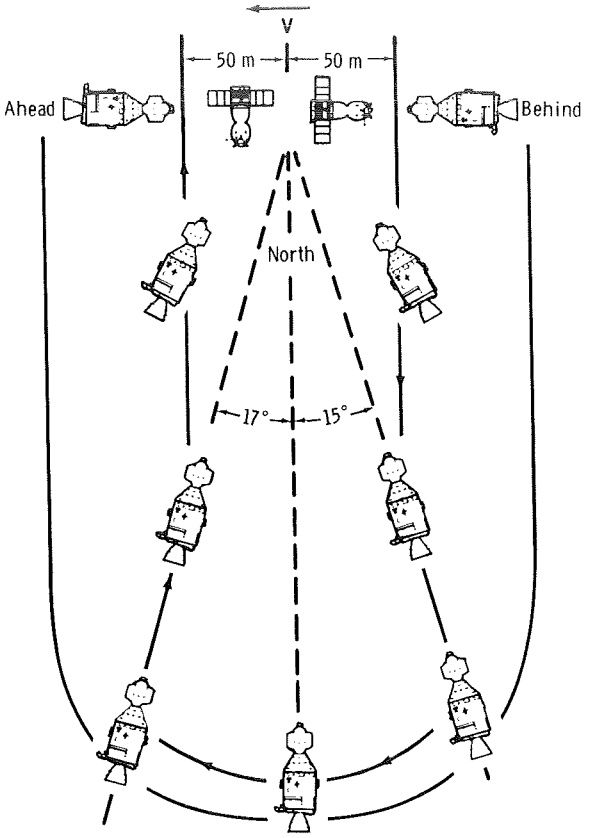

FIGURE 8-9.—Illustration of the 500-m out-of-plane data take.

maneuvered, as shown in the figure, to a position 500 m from the Soyuz vehicle out of the orbital plane and 15° behind. The Apollo vehicle then executed a circular sweep through 32° (−15° to +17°) in a horizontal plane that contained the Soyuz vehicle; the maneuver required 10 minutes. Very early in this maneuver, clear indication was obtained in all UV channels that reflected radiation was being received by the UVA spectrometer. Reflected data were received (as indicated in the 135.6-nm channel) throughout the sweep. Figure 8-10 is an example of the strip-chart records showing a complete spectral scan taken during the sweep for comparison with a spectrum obtained from the UVA door just before the sweep (fig. 8-11). The observed ratio of the counting rates at 130.4 and 135.6 nm was 5.7 ± 0.5 from 101:17:38.13 to 101:17:40.25 GET. (The sweep began at 101:17:37 GET.) The ratio obtained from the door (after correction for the reflectivity of the door) was 5.72. The ratio of 130.4 to 135.6 nm obtained during the run is shown in figure 8-12. There was an anomaly during the run; the 135.6-nm counting rate dropped by a factor of 5.5 from a plateau of about 250 counts to about 45 counts between 101:17:39.37 and 101:17:41.49 GET. It remained at 45 counts thereafter. A similar effect occurred in the 149.3-nm channel. These anomalies are being analyzed.

During the warmup period for the next eclipse pass, the signals reflected from the door were normal during the first several minutes; this observation indicates that no change in the lamp output, collimating mirror reflectivity, or receiver *QT* was responsible for the drop in signal during the second part of the 500-m pass. However, the calibration signal dropped by a factor of approximately 4 in all channels during the last several minutes of the warmup period and remained low after the door was opened for the 1000-m data take. As shown in figure 8-13, these data were obtained in the orbital plane during separation of the Apollo and Soyuz vehicles. The upward-looking retroreflector was used, and the range varied from 800 to 1300 m during the sweep from +15° to −15° with the vertical.

Some reflected signals were detected, although the retroreflector was only in the field of view sporadically. Use of the COAS and the star tracker was very difficult because bright moonlight was illuminating the top of the Soyuz spacecraft. An attempt was made to use the COAS to keep the Apollo vehicle pointed toward the Soyuz beacon and navigation lamps instead of trying to lock on the retroreflector as in the out-of-plane observations.

After the Apollo departed the neighborhood of the Soyuz, two resonance exercises were performed. During an eclipse phase, the Apollo X-axis was oriented normal to the orbital plane and one full orbit (from 105:10 to106:46 GET) of resonance fluorescence and airglow background data was obtained. This exercise was followed during the next eclipse phase (from 106:55 to 107:10 GET) with an observation of the resonance fluorescence signal obtained with the Apollo X-axis still oriented normal to the orbital plane and with the Apollo vehicle executing a slow roll through 360°. The purpose of this exercise was to

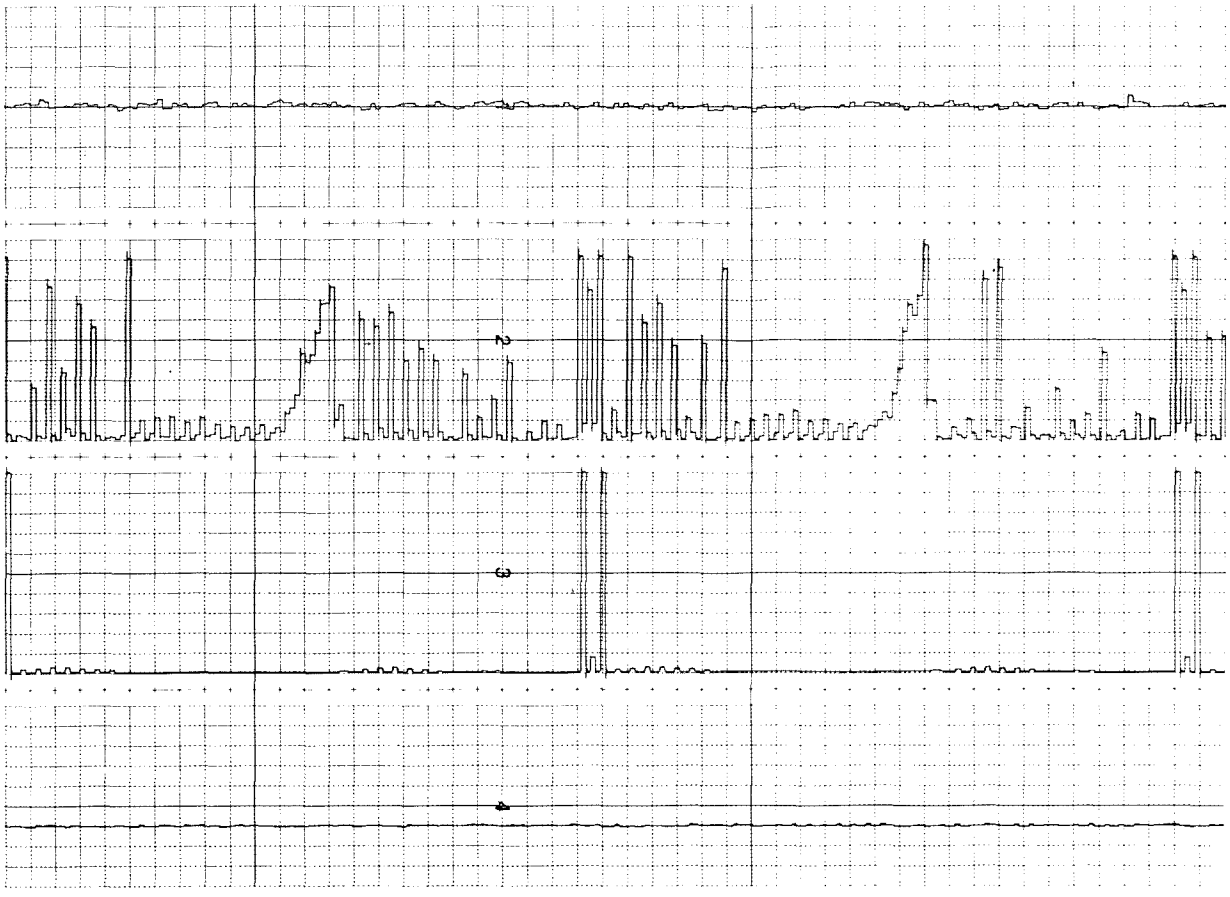

FIGURE 8-10.—Strip-chart record taken during the 500-m data take.

determine the variation in population of thermal O atoms between the ram side of the docking module and the lee side (fig. 8-14). The atoms near the aperture consist of ambient undisturbed atmosphere and atoms that have been scattered from the vehicle. Obviously, the higher density will be on the ram side of the vehicle. Some of the atoms striking the vehicle will have become thermalized, and then reflect. Some will recombine and become O_2 molecules. The recombining fraction should be determinable from the data obtained, because the 130.4-nm fluorescence signal was found to depend strongly on the roll orientation.

The resonance fluorescence counting rate was expected to be approximately 3.5×10^4 counts/sec at $\theta = 0°$ and approximately 10^4 counts/sec at $\theta = 10°$ if the oxygen density was 10^9 cm^{-3}. The transmitted signal was expected to be approximately 3×10^4 counts/sec at $\theta = 0°$ and approximately 7.5×10^4 counts/sec at $\theta = 10°$ for the same density. These were the values predicted when the spacecraft velocity was 7.8 km/sec and the O temperature was 777 K, as they were during the flight. The temperature was determined from the 10.7-cm solar flux and the A_p index (measurement of magnetic activity at the poles).

If it is assumed that during the 150-m data take all the signal was due to resonance fluorescence, the observed counting rates of only approximately 5.8×10^3 counts/sec at $\theta = 0°$ are approximately a factor of 6 lower than expected. Similarly, if a presumed contribution of 5.8×10^3 counts/sec from resonance fluorescence is subtracted from a counting rate of approximately 7×10^3 counts/sec at $\theta = 0°$ during the 500-m data take, the result (1.1×10^3 counts/sec) is too low by a

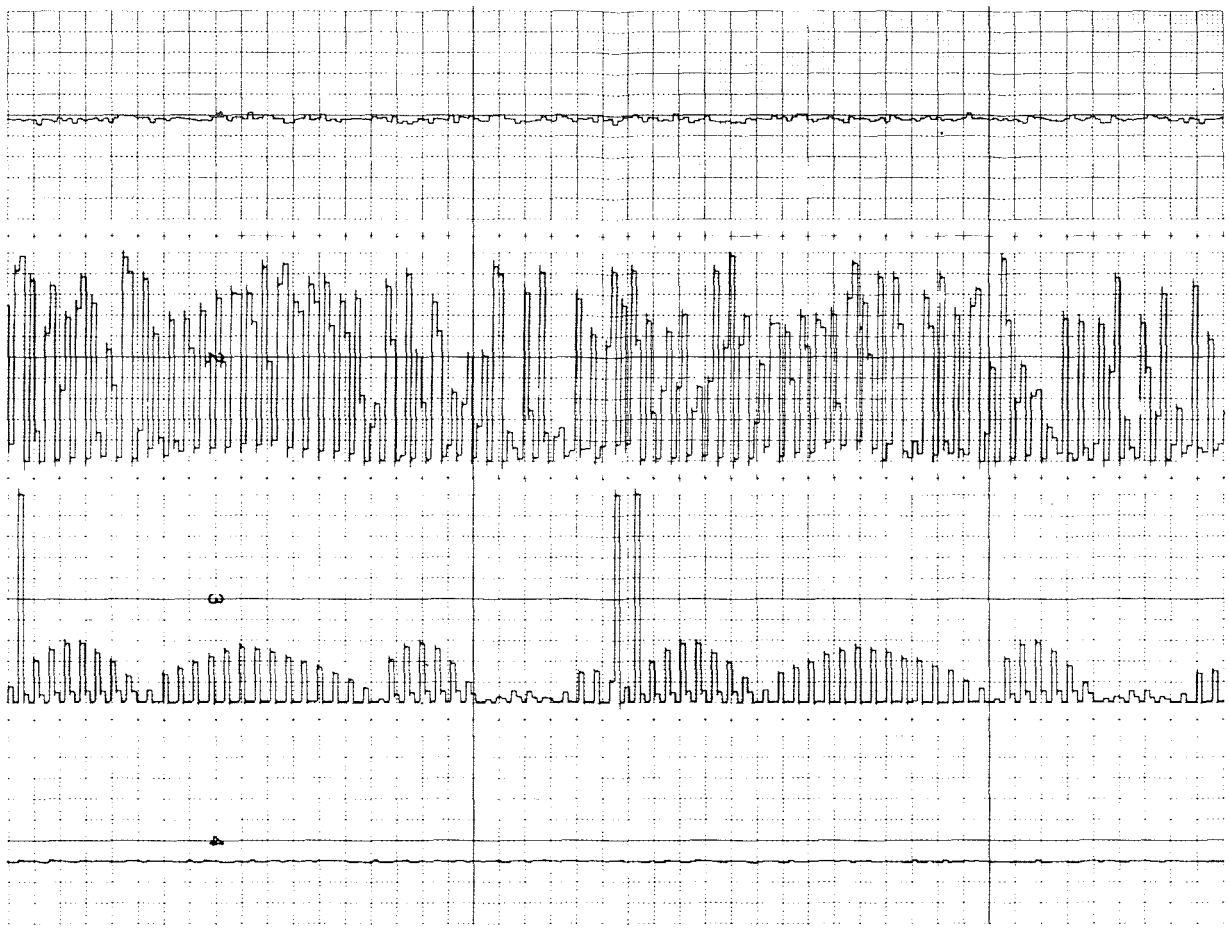

FIGURE 8-11.—Strip-chart record taken just before the 500-m data take.

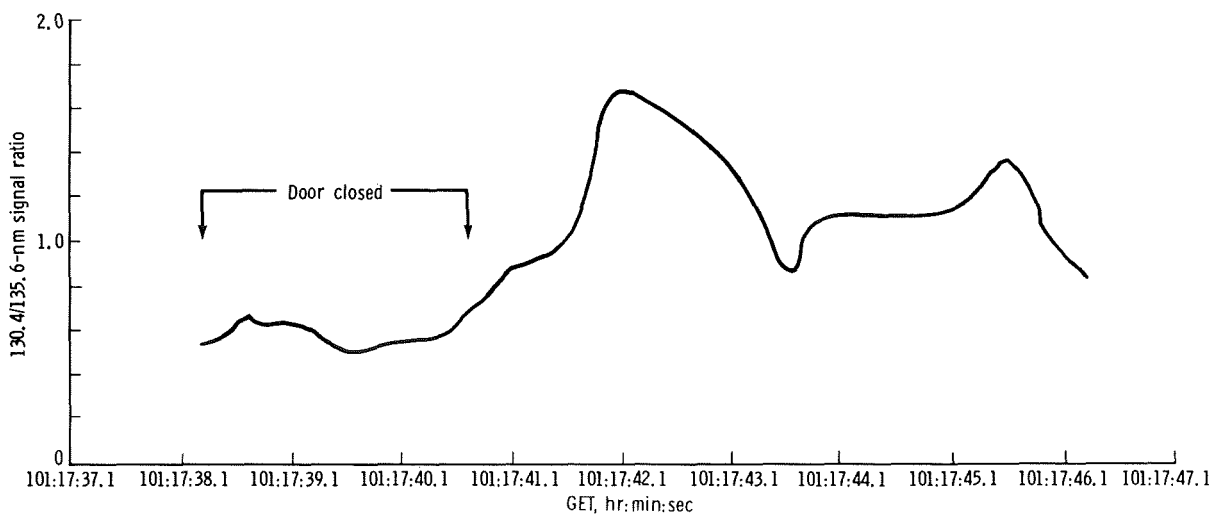

FIGURE 8-12.—Ratio of the 130.4- to 135.6-nm signal during the 500-m data take.

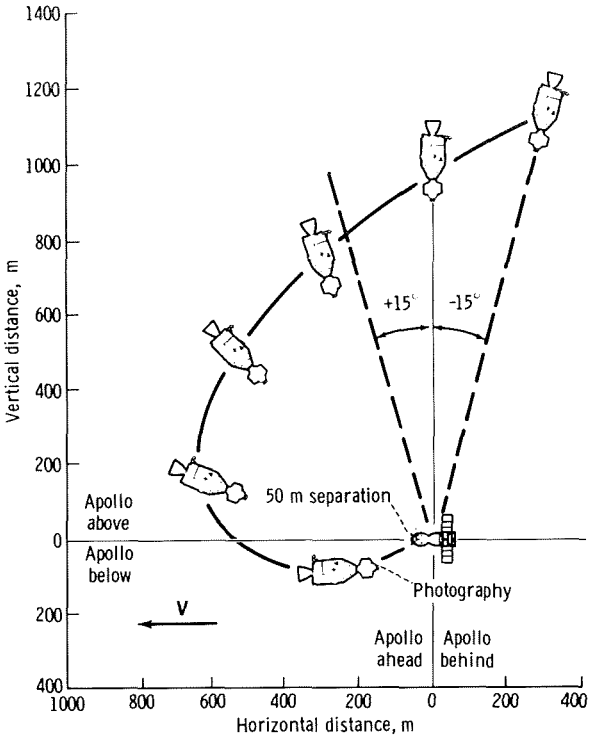

FIGURE 8-13.—Illustration of the 1000-m in-plane data take.

factor of 25. Even if the degradation in the 135.6- and 149.3-nm signals is presumed to indicate a drop in reflectivity of the retroreflector by a factor of 2500/500 (or 5) between the beginning of the data take and the time θ reached 0°, the corrected counting rate becomes 6×10^3 counts/sec. This value is still approximately a factor of 5 lower than expected. The conclusion is that, for reasons unknown, the radiance in the beam leaving the collimating mirror was lower than expected by a factor of approximately 5. Thus, the data have been analyzed inferring relative values only.

Counting rates as a function of θ obtained during the 150- and the 500-m data takes are displayed in figure 8-15. An unexpected lack of symmetry exists about $\theta = 0°$ in the case of the 130.4-nm signal during the 150-mm data take. Although the variation with θ for $\theta < 0$ resembles that expected for pure resonance fluorescence, the counting rate remains almost independent of θ as the latter increases toward high positive values. The data obtained during the 360° roll maneuver executed later in the flight show a very significant increase in fluorescence caused by atom pileup on the ram side of the spacecraft. As shown in figure 8-8, during the period when θ was negative, the field of view of the spectrometer was entirely in the wake, whereas during the period when θ was positive, a portion of atmosphere on the ram side of the spacecraft was in the field of view. This is believed to be responsible for the asymmetry.

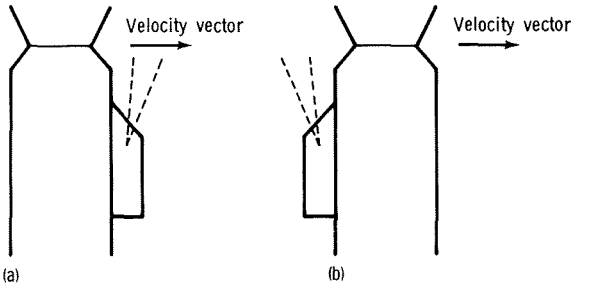

FIGURE 8-14.—Collecting aperture orientation on Apollo docking module. (a) Ram side. (b) Lee side.

The investigators have assumed that, during the 150-m data take, the signal was caused entirely by resonance fluorescence, whereas the 500-m data contain contributions from reflection and fluorescence. To obtain the variation of transmitted signal with θ, the fluorescence contribution has been assumed to the same during the 500-m data take as it was during the 150-m data take for the same values of θ. As suggested by the calibration data taken after the 500-m data take, it was also assumed that the decrease in signal during the 500-m pass was caused by deterioration of the corner reflectors. Hence, it can be corrected by use of the 135.6-nm signal. Figure 8-16 is a plot of the resonance absorption signal S as a function of θ where $S(\theta)$ is calculated as follows:

$$S(\theta) = \left[R_{130.4}(\theta, 500\text{ m}) - R_{130.4}(\theta, 150\text{ m})\right] \left[\frac{2500}{R_{135.6}(\theta, 500\text{ m})}\right] \tag{8-9}$$

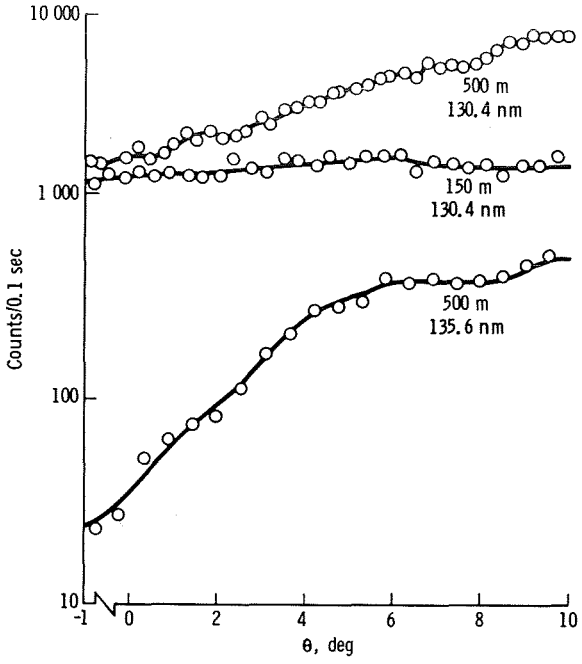

FIGURE 8-15.—Counts/0.1 sec obtained at 130.4 nm during the 150-m data take and at 130.4 nm and 135.6 nm during the 500-m data take.

where R represents the measured counting rates. Because R at 135.6 nm remained constant at 2500 counts/sec until θ reached 6°, it was assumed that this rate represented the unperturbed 135.6-nm counting rate.

The results have been analyzed in several ways. In figure 8-16, curves showing the theoretical variation in counting rate with θ in arbitrary units can be compared with the observed values of $S(\theta)$. A least-squares fit of theoretical $S(\theta)$ curves with the data indicates a value for the oxygen density of

$$[O] = (1.2 \pm 0.5) \times 10^9 \text{ cm}^{-3} \qquad (8\text{-}10)$$

On the other hand, because the data between θ values of 4° and 8° show much less scatter than those obtained at large θ (when the lamps were still coming into a steady state) and at small θ (when the reflected signal was low), a fit of $S(\theta)$ to the observed data for $4° < \theta < 8°$ gives

$$[O] = (1.15 \pm 0.36) \times 10^9 \text{ cm}^{-3} \qquad (8\text{-}11)$$

Finally, it is appropriate to compare the resonance fluorescence signal S_R to the transmitted signal S_T for consistency. The ratio of S_R at $\theta = 0°$ and S_T for any value of θ (for instance, 8°) is a unique function of [O]. The observed value for $S_R(0°)/S_T(8°)$ indicates a value for the oxygen density

$$[O] = (1.15 \pm 0.06) \times 10^9 \text{ cm}^{-3} \qquad (8\text{-}12)$$

In summary, the experiment results predict

$$[O] = (1.15 \pm 0.2) \times 10^9 \text{ cm}^{-3} \qquad (8\text{-}13)$$

In the case of N, the 149.3-nm reflected line experienced the same degradation with θ as the 135.6 [O] line. During the 150-m data take, the resonance fluorescence counting rate at 120 nm was only 6.1 ± 1.3 counts/sec. During the 500-m data take, no significant variation in the transmitted 120.0-nm signal could be seen after a correction was made for the variation in the 149.3-nm counting rate. The value of S_T was 400 ± 68 counts/sec. For the nitrogen density [N], the ratio of S_T to S_R of 66 ± 18 gives

$$[N] = \left(8.6 \begin{smallmatrix} +2.7 \\ -1.7 \end{smallmatrix}\right) \times 10^6 \text{ cm}^{-3} \qquad (8\text{-}14)$$

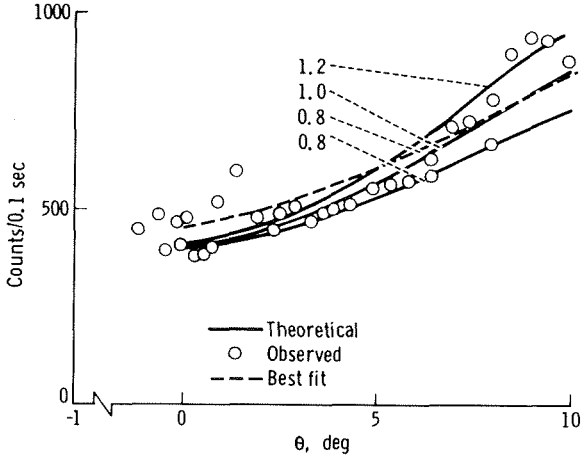

FIGURE 8-16.—Counts/0.1 sec obtained by equation (8-9) compared to theory in units of 10^9 oxygen atoms/cm^3. (Numbers indicate the assumed oxygen densities.)

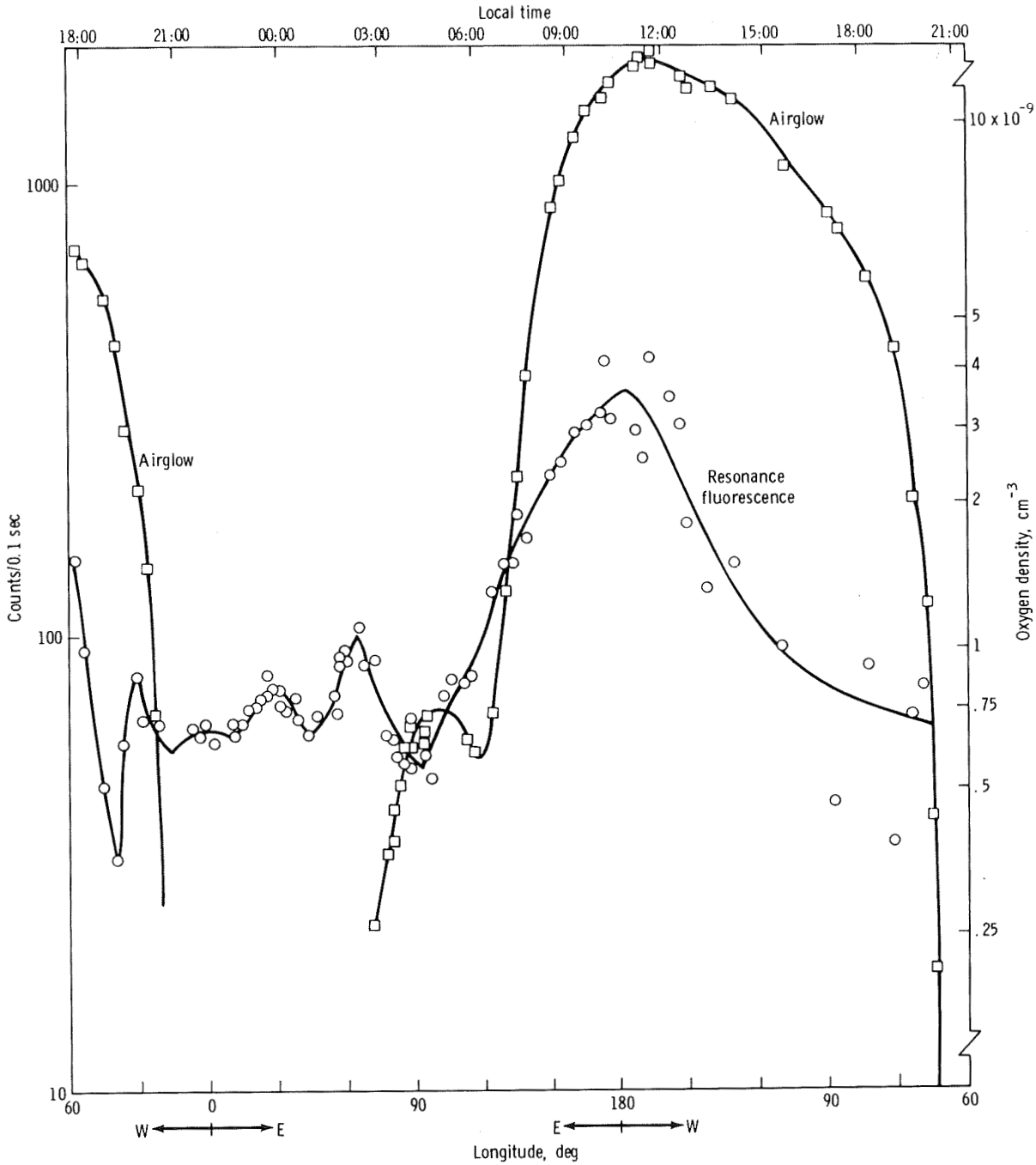

FIGURE 8-17.—The 130.4-nm resonance fluorescence and atomic oxygen density inferred from it during an entire orbit. The 130.4-nm airglow counting rate is also plotted.

The data obtained during the resonance fluorescence/airglow orbit (105:10 to 106:46 GET) are shown in figure 8-17. Correcting for the 6.7-fold decrease in sensitivity that occurred just before the 1000-m data take, the oxygen densities inferred are indicated as well. The oxygen airglow component was obtained from the signal at 130.4 nm when no lamp was illuminated. The apparent increase in ambient oxygen density during the day is inconsistent with what is known about the atmosphere at 225 km. This inconsistency is attributed to atoms that somehow had outgassed from the Apollo vehicle when it was in sunlight. It is significant that the maximum apparent density occurred when the Sun was at local noon.

Twice during this orbit (22:30 local time and latitude 10° N, 10:30 local time and latitude 10° S), the Apollo passed under Atmosphere Explorer (AE), which was at a 340-km altitude. Extrapolating the AE oxygen density to 234 km (which was the altitude of Apollo at 22:30 local time) by means of the Orbiting Geophysical Observatory 6 model would give 1.0×10^9 cm^{-3} for the density. The Apollo resonance fluorescence value was 0.92×10^9 cm^{-3}. At latitude 10° S, 10:30 local time, the AE extrapolation called for 1.32×10^9 cm^{-3} and the fluorescence value was 4.8×10^9 cm^{-3}. During the 500-m data take, AE was at latitude 35° S and the local time was 08:00. The oxygen density extrapolated to Apollo altitude was 1.5×10^9 cm^{-3}. The agreement between the AE measurements and those of this experiment is considered to be quite satisfactory.

The results of the 360° roll maneuver were that the apparent oxygen density varied from approximately 0.46×10^9 cm^{-3} in the wake to 4.3×10^9 cm^{-3} in the ram direction, which showed the extreme enhancement of density caused by the reflection of atmospheric gas from the spacecraft.

REFERENCES

8-1. Philbrick, C. R.; and McIsaac, J. P.: Measurements of Atmospheric Composition Near 400 KM. Space Research XII, vol. 1, Academie-Verlag (Berlin), 1972, pp. 743-749.

8-2. Ghosh, S. N.; Hinton, B. B.; et al.: Atomic Nitrogen in the Upper Atmosphere Measured by Mass Spectrometers. J. Geophys. Res., vol. 73, no. 13, July 1968, pp. 4425-4426.

8-3. Hickman, David R.; and Nier, Alfred O.: Measurement of the Neutral Composition of the Lower Thermosphere Above Fort Churchill by Rocket-Borne Mass Spectrometer. J. Geophys. Res., vol. 77, no. 16, June 1972, pp. 2880-2887.

8-4. Fastie, William G.; Feldman, Paul D.; et al.: A Search for Far-Ultraviolet Emissions From the Lunar Atmosphere. Science, vol. 182, no. 4113, Nov. 1973, pp. 710-711.

8-5. Lin, Chorng-Lieh; Parkes, David A.; and Kaufman, Frederick: Oscillator Strength of the Resonance Transitions of Ground-State N and O. J. Chem. Phys., vol. 53, no. 10, Nov. 1970, pp. 3896-3900.